THE JOURNAL OF PHYSICAL CHEMISTRY C

Article

pubs.acs.org/JPCC

NMR Study of Reorientational Motion in Alkaline-Earth Borohydrides: β and γ Phases of $Mg(BH_4)_2$ and α and β Phases of $Ca(BH_4)_2$

Alexei V. Soloninin,[†] Olga A. Babanova,[†] Alexander V. Skripov,*[,†] Hans Hagemann,[‡] Bo Richter,[§] Torben R. Jensen,[§] and Yaroslav Filinchuk*[,∥]

[†]Institute of Metal Physics, Ural Division of the Russian Academy of Sciences, S. Kovalevskoi 18, Ekaterinburg 620041, Russia

[‡]Département de Chimie Physique, Université de Genève, 30 Quai Ernest Ansermet, 1211 Genève, Switzerland

[§]Center for Materials Crystallography, Interdisciplinary Nanoscience Center and Department of Chemistry, Aarhus University, Langelandsgade 140, 8000 Aarhus C, Denmark

[∥]Institute of Condensed Matter and Nanosciences, Université Catolique de Louvain, Place L. Pasteur 1, 1348 Louvain-la-Neuve, Belgium

ABSTRACT: To study the reorientational motion of BH_4 groups in β and γ phases of $Mg(BH_4)_2$ and in α and β phases of $Ca(BH_4)_2$, we have performed nuclear magnetic resonance (NMR) measurements of the ^1H and ^{11}B spin–lattice relaxation rates in these compounds over wide ranges of temperature and resonance frequency. It is found that at low temperatures the reorientational motion in β phases of $Mg(BH_4)_2$ and $Ca(BH_4)_2$ is considerably faster than in other studied phases of these alkaline-earth borohydrides. The behavior of the measured spin–lattice relaxation rates in both β phases can be satisfactorily described in terms of a Gaussian distribution of activation energies E_a with the average E_a values of 138 meV for β-$Mg(BH_4)_2$ and 116 meV for β-$Ca(BH_4)_2$. The α phase of $Ca(BH_4)_2$ is characterized by the activation energy of 286 ± 7 meV. For the novel porous γ phase of $Mg(BH_4)_2$, the main reorientational process responsible for the observed spin–lattice relaxation rate maximum can be described by the activation energy of 276 ± 5 meV. The barriers for reorientational motion in different phases of alkaline-earth borohydrides are discussed on the basis of changes in the local environment of BH_4 groups.

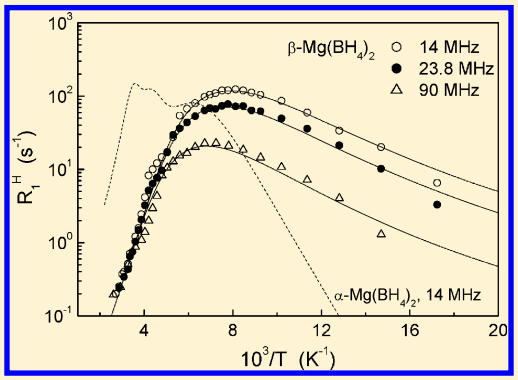

INTRODUCTION

The alkaline-earth tetrahydroborates (borohydrides) $Mg(BH_4)_2$ and $Ca(BH_4)_2$ are considered as promising materials for hydrogen storage.[1−3] Both compounds have high gravimetric hydrogen content (14.9 and 11.5 wt %, respectively), and their hydrogen desorption temperatures are lower than for alkali borohydrides, such as $LiBH_4$ and $NaBH_4$. Furthermore, the dehydrogenation–hydrogenation reaction in both $Mg(BH_4)_2$ and $Ca(BH_4)_2$ has been shown to be partially reversible.[4−6] Elucidation of the crystal structures and hydrogen dynamics in these compounds may give a key to improving their hydrogen-storage properties.

X-ray[7−9] and neutron diffraction[7] studies of the crystal structures of $Mg(BH_4)_2$ have revealed an unexpected structural complexity of this material. The unit cell of the low-temperature hexagonal (α) phase of $Mg(BH_4)_2$ (space group $P6_122$)[9] contains 330 atoms. It is interesting to note that the structure of α-$Mg(BH_4)_2$ includes unoccupied voids,[9] each of the volume of 37 Å^3. Above 490 K, α-$Mg(BH_4)_2$ irreversibly transforms to the orthorhombic high-temperature (β) phase (space group $Fddd$),[8,9] the unit cell of which contains 704 atoms. Recently, two new phases of $Mg(BH_4)_2$ have been discovered:[10] the cubic γ phase (space group $Id\bar{3}a$) and the tetragonal δ phase (space group $P4_2nm$). The characteristic feature of the γ phase is a three-dimensional set of interpenetrating channels. The empty volume in the structure of the γ phase amounts to 33%, which makes γ-$Mg(BH_4)_2$ the first hydride with high permanent porosity. Due to such a porosity, γ-$Mg(BH_4)_2$ can adsorb guest molecules of CH_2Cl_2, N_2, and H_2.[10] Thus, γ-$Mg(BH_4)_2$ can store hydrogen both in the form of $[BH_4]^-$ groups and in adsorbed molecular form. The tetragonal δ phase of $Mg(BH_4)_2$ is formed from α-$Mg(BH_4)_2$ at moderate pressures of 1.1–1.6 GPa. The δ phase has the highest density among all known phases of $Mg(BH_4)_2$; this phase is found to retain its stability after the pressure release at ambient conditions.[10] Four different crystalline phases have also been reported for $Ca(BH_4)_2$.[2,11−13] The low-temperature orthorhombic α phase (space group $F2dd$) exhibits a second-order transition to the closely related tetragonal α' phase (space group $I\bar{4}2d$)[12] at ~495 K. Both α and α' phases start to transform kinetically into a completely different β phase above 450 K, and this transformation becomes very fast above 550 K. Determination of the space group symmetry of

Received: November 2, 2011
Revised: January 30, 2012
Published: January 31, 2012

β-$Ca(BH_4)_2$ is ambiguous, and its structure was described by space groups $P4_2/m$ (ref 11) and $P\bar{4}$ (ref 12). It is likely that the BH_4 groups in this phase are intrinsically disordered. The high-temperature β phase of $Ca(BH_4)_2$ is metastable on cooling, and at room temperature it slowly transforms back to the α phase.[14] Another phase, γ-$Ca(BH_4)_2$, obtained by wet chemical synthesis has an orthorhombic structure;[13] it remains metastable at all temperatures and irreversibly transforms to the β phase at ~590 K.

Microscopic information on hydrogen dynamics can be obtained from nuclear magnetic resonance (NMR) and quasielastic neutron scattering (QENS) measurements. The first NMR study of reorientational motion in an alkaline-earth borohydride has revealed a coexistence of at least three jump processes in α-$Mg(BH_4)_2$.[15] Taking into account the anisotropy of the local environment of BH_4 groups in α-$Mg(BH_4)_2$, these jump processes have been attributed to different types of BH_4 reorientations.[15] NMR was also applied to study the atomic motion in β-$Mg(BH_4)_2$, ball-milled α-$Mg(BH_4)_2$ with TiF_3 and $ScCl_3$ additives, and α-$Mg(BH_4)_2$ incorporated into carbon aerogel.[16] This work has revealed a significant difference between the reorientational motion in bulk α and β phases of $Mg(BH_4)_2$; however, because of the limited experimental temperature range and the use of a single resonance frequency, the reorientational motion in β-$Mg(BH_4)_2$ could not be fully characterized.[16] Hydrogen jump motion in β-$Ca(BH_4)_2$ was investigated by QENS measurements;[17] the results were consistent with two coexisting types of reorientational motion (BH_4 reorientations around 2-fold and 3-fold axes) and a slower long-range diffusion process involving some unidentified H-containing species. The results of the recent QENS study[18] of β-$Mg(BH_4)_2$ were consistent with three coexisting types of BH_4 reorientations. The aim of the present work is to investigate the H jump motion in four phases of alkaline-earth borohydrides (β and γ phases of $Mg(BH_4)_2$ and α and β phases of $Ca(BH_4)_2$) using ^{1}H and ^{11}B NMR measurements of the spectra and spin–lattice relaxation rates over wide ranges of temperature (18–426 K) and resonance frequency (14–90 MHz).

EXPERIMENTAL METHODS

The β phase of $Mg(BH_4)_2$ was prepared by annealing the sample of α-$Mg(BH_4)_2$ used in our previous work[15] at 240 °C. The preparation of the nanoporous cubic γ phase of $Mg(BH_4)_2$ was described in ref 10. According to X-ray diffraction analysis, the sample of γ-$Mg(BH_4)_2$ was single-phase with the lattice parameter a = 15.7575(16) Å. The low-temperature modification of $Ca(BH_4)_2$ was prepared using the procedure analogous to that described in ref 12. According to X-ray diffraction analysis, in addition to the α phase, this sample contained about 13% of β-$Ca(BH_4)_2$. In the following, this sample will be referred to as "α-$Ca(BH_4)_2$". To obtain the high-temperature (β) modification of $Ca(BH_4)_2$, we annealed this sample at 260 °C for 2 h. The resulting sample will be referred to as "β-$Ca(BH_4)_2$", although, as it will be shown below, the $\alpha \rightarrow \beta$ transformation was not complete. For NMR experiments, all the samples were sealed in glass tubes under ~500 mbar of nitrogen gas.

NMR measurements were performed on a modernized Bruker SXP pulse spectrometer with quadrature phase detection at the frequencies $\omega/2\pi$ = 14 (or 14.5), 23.8, and 90 MHz for ^{1}H and 14 and 28 MHz for ^{11}B. The magnetic field was provided by a 2.1 T iron-core Bruker magnet. A home-built multinuclear continuous-wave NMR magnetometer working in the range 0.32–2.15 T was used for field stabilization. For rf pulse generation, we used a home-built computer-controlled pulse programmer, the PTS frequency synthesizer (Programmed Test Sources, Inc.), and a 1 kW Kalmus wideband pulse amplifier. Typical values of the $\pi/2$ pulse length were 2–3 μs for both ^{1}H and ^{11}B. A probehead with the sample was placed into an Oxford Instruments CF1200 continuous-flow cryostat using helium or nitrogen as a cooling agent. The sample temperature, monitored by a chromel-(Au–Fe) thermocouple, was stable to ±0.1 K. The nuclear spin–lattice relaxation rates were measured using the saturation–recovery method. NMR spectra were recorded by Fourier transforming the spin echo signals.

RESULTS AND DISCUSSION

1. β and γ Phases of $Mg(BH_4)_2$. The temperature dependences of the proton spin–lattice relaxation rates R_1^H measured at three resonance frequencies for β-$Mg(BH_4)_2$ are shown in Figure 1. As typical of the relaxation mechanism

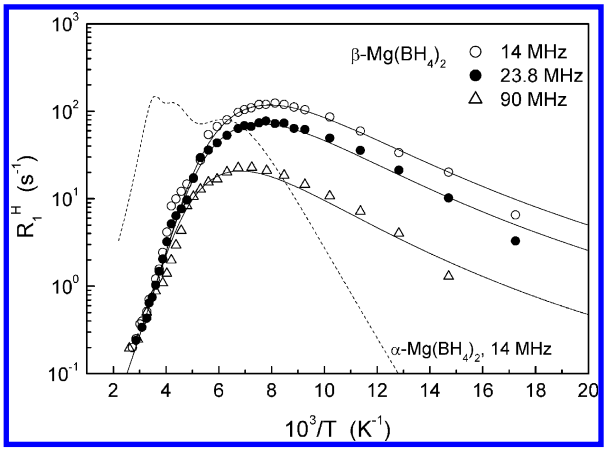

Figure 1. Proton spin–lattice relaxation rates measured at 14, 23.8, and 90 MHz for β-$Mg(BH_4)_2$ as functions of the inverse temperature. The solid lines show the simultaneous fits of the model with a Gaussian distribution of the activation energies to the data. The dashed line shows the fit of the "three-peak" model to the data for α-$Mg(BH_4)_2$ at 14 MHz (ref 15).

due to nuclear dipole–dipole interaction modulated by atomic motion,[19] $R_1^H(T)$ exhibits a frequency-dependent maximum. This maximum is expected to occur at the temperature at which the atomic jump rate τ^{-1} becomes nearly equal to the resonance frequency ω. Similar maxima originating from reorientations of the BH_4 groups were observed for the other studied borohydrides.[20−27] Our R_1^H results at $\omega/2\pi$ = 90 MHz (Figure 1) are close to those reported by Shane et al.[16] for β-$Mg(BH_4)_2$ at 85 MHz. It should be noted, however, that the proton relaxation rate measurements in ref 16 were performed only down to 120 K; i.e., the low-temperature slope of the $R_1^H(T)$ peak was not observed at all. According to the standard theory[19] of nuclear spin–lattice relaxation due to atomic motion with a single jump rate τ^{-1}, in the limit of slow motion ($\omega\tau \gg 1$), R_1^H should be proportional to $\omega^{-2}\tau^{-1}$, and in the limit of fast motion ($\omega\tau \ll 1$), R_1^H should be proportional to τ being frequency-independent. If the temperature dependence of τ^{-1} is governed by the Arrhenius law with the activation energy E_a

$$\tau^{-1} = \tau_0^{-1} \exp(-E_a/k_B T) \quad (1)$$

a plot of ln R_1^H vs T^{-1} should be linear in the limits of both slow and fast motion with the slopes $-E_a/k_B$ and E_a/k_B, respectively. As can be seen from Figure 1, for β-$Mg(BH_4)_2$ the

dx.doi.org/10.1021/jp210509g | J. Phys. Chem. C 2012, 116, 4913–4920

high-temperature slope of such a plot is considerably steeper than the low-temperature slope. Moreover, the experimental frequency dependence of R_1^H at the low-temperature slope is much weaker than the expected ω^{-2} dependence. These features are consistent with the presence of a broad distribution of H jump rates.[28] Such a distribution can also be parametrized in terms of a distribution of the activation energies. The simplest model is based on a Gaussian distribution of E_a values.[28] For this model, the observed spin−lattice relaxation rate is expressed as

$$R_1^H = \int R_1^H(E_a) G(E_a) dE_a \quad (2)$$

where $G(E_a)$ is a Gaussian distribution of the activation energies, and $R_1^H(E_a)$ is given by

$$R_1^H(E_a) = \frac{\Delta M_{HB}\tau}{2}\left[\frac{1}{1+(\omega_H-\omega_B)^2\tau^2} + \frac{3}{1+\omega_H^2\tau^2} + \frac{6}{1+(\omega_H+\omega_B)^2\tau^2}\right] + \frac{4\Delta M_{HH}\tau}{3} \times \left[\frac{1}{4+\omega_H^2\tau^2} + \frac{1}{1+\omega_H^2\tau^2}\right] \quad (3)$$

and eq 1. Here ω_H and ω_B are the resonance frequencies of ^{1}H and ^{11}B, respectively, and ΔM_{HB} and ΔM_{HH} are the parts of the dipolar second moment due to H−B and H−H interactions that are caused to fluctuate by the reorientational motion. Our estimates show that ^{1}H−^{25}Mg dipole−dipole interactions can be neglected. The parameters of the model are ΔM_{HB}, ΔM_{HH}, τ_0, the average activation energy $\bar{E}_a$, and the width of the distribution (dispersion) ΔE_a. These parameters can be varied to find the best fit to the $R_1^H(T)$ data at the three resonance frequencies simultaneously. Since the H−B and H−H terms in eq 3 show nearly the same temperature and frequency dependences, it is practically impossible to determine the amplitude parameters ΔM_{HB} and ΔM_{HH} independently from the fits. The estimates for alkali-metal borohydrides[24,26] indicate that ΔM_{HB} and ΔM_{HH} are close to each other. Therefore, for parametrization of the R_1^H data we shall assume that $\Delta M_{HB} = \Delta M_{HH} \equiv \Delta M$. The results of the simultaneous fit of the model with a Gaussian distribution of activation energies (eqs 2, 3, and 1) to the data are shown by solid curves in Figure 1. It can be seen that this simple model satisfactorily describes the experimental data over wide ranges of temperature and resonance frequency. The corresponding values of the fit parameters are $\Delta M = (9.6 \pm 0.2) \times 10^9$ s^{-2}, $\tau_0 = (1.6 \pm 0.4) \times 10^{-14}$ s, $\bar{E}_a = 138 \pm 5$ meV, and $\Delta E_a = 36 \pm 3$ meV. It should be noted that the value of $\bar{E}_a$ resulting from this fit is close to the activation energy (123 meV) derived by Shane et al.[16] from the high-temperature slope of the $R_1^H(T)$ peak for β-$Mg(BH_4)_2$. The results of recent QENS measurements[18] for β-$Mg(BH_4)_2$ were interpreted in terms of three reorientational processes with different E_a values, although the authors[18] could not exclude the possibility of a more complex distribution of the activation energies. The faster jump processes with the activation energies of 39 and 76 meV were attributed to reorientations of inequivalent BH_4 groups around the 2-fold axes nearly parallel to the lines connecting two nearest-neighbor Mg atoms; the process with E_a = 39 meV was found to have a low weight (~0.15).[18] The slower jump process with the activation energy of 214 meV was ascribed to BH_4 reorientations around the 3-fold axes. The weighted average E_a value for the 2-fold and 3-fold reorientations[18] is 142 meV, which is close to our $\bar{E}_a$ value for β-$Mg(BH_4)_2$. However, our $R_1^H(T)$ results for β-$Mg(BH_4)_2$ do not resolve separate contributions from the 2-fold and 3-fold reorientations; possible reasons for that will be discussed below in relation with the results for β-$Ca(BH_4)_2$. To compare the behavior of the proton spin−lattice relaxation rates in α and β phases of $Mg(BH_4)_2$, we have also included in Figure 1 the results of our fit to the $R_1^H(T)$ data for α-$Mg(BH_4)_2$ at $\omega/2\pi$ = 14 MHz.[15] As can be seen from Figure 1, the $R_1^H(T)$ peak for β-$Mg(BH_4)_2$ is shifted to considerably lower temperatures with respect to both $R_1^H(T)$ peaks for α-$Mg(BH_4)_2$. This means that the reorientational motion of BH_4 groups in the β phase is generally much faster than in the α phase. More precisely, the distribution of H jump rates in the β phase is shifted to higher rates with respect to that in the α phase. The significant value of ΔE_a for β-$Mg(BH_4)_2$ may result from the antisite disorder[8] and the considerable spread in B−Mg distances. In fact, the B−Mg distances in the β phase show a broader distribution (2.34−2.49 Å from the experiment[8] and 2.36−2.44 Å from the DFT calculations[29]) than in the α phase (2.400−2.437 Å from the single-crystal data[9] and 2.382−2.416 Å from the DFT calculations[29]) and in the γ phase (a single distance of 2.413(3) Å).[10]

For γ-$Mg(BH_4)_2$, we have performed NMR measurements only up to 320 K since at higher temperatures this phase is known to lose its stability.[10] Figure 2 shows the results of the $R_1^H(T)$ measurements for γ-$Mg(BH_4)_2$ at three resonance frequencies. As can be seen from this figure, the proton relaxation rate exhibits a frequency-dependent peak near room temperature. The high-temperature slope of this peak has not been observed in our measurements; this feature does not allow us to perform a full analysis of the $R_1^H(T)$ data. The low-temperature slope of the $R_1^H(T)$ peak strongly deviates from the linear behavior in coordinates log $R_1^H - T^{-1}$ (Figure 2). Furthermore, the frequency dependence of the proton relaxation rate at the low-temperature slope appears to be considerably weaker than the expected ω^{-2} dependence. These features suggest the presence of a broad (evidently, two-peak) distribution of H jump rates. It should be noted that all H jump processes contributing to the observed behavior of $R_1^H(T)$ correspond to

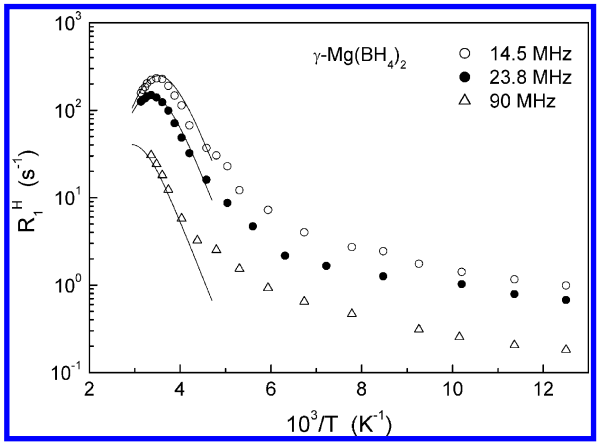

Figure 2. Proton spin−lattice relaxation rates measured at 14.5, 23.8, and 90 MHz for γ-$Mg(BH_4)_2$ as functions of the inverse temperature. The solid lines show the simultaneous fits of the model with a Gaussian distribution of the activation energies to the data in the range 230−320 K.

dx.doi.org/10.1021/jp210509g | J. Phys. Chem. C 2012, 116, 4913−4920

reorientational (localized) motion. This is supported by the temperature dependence of the ^{1}H NMR line width. Figure 3

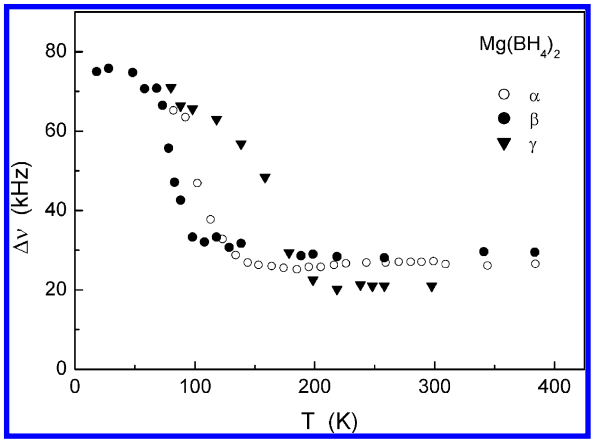

Figure 3. Temperature dependences of the width (full width at half-maximum) of the proton NMR spectra measured at 23.8 MHz for α (ref 15), β, and γ phases of $Mg(BH_4)_2$.

shows the temperature dependences of the full width at half-maximum, $\Delta\nu$, of the ^{1}H NMR spectra for β and γ phases of $Mg(BH_4)_2$; for comparison, the corresponding results for α-$Mg(BH_4)_2$ (ref 15) are also included. For all these phases, the observed line narrowing indicates the excitation of H jump motion on the frequency scale of the order of 10^5 s^{-1}. For β-$Mg(BH_4)_2$, the sharp drop in $\Delta\nu$ occurs at the lowest temperature (~80 K) among the studied phases of $Mg(BH_4)_2$; this is consistent with the fastest H jump motion in the β phase. For γ-$Mg(BH_4)_2$, the region of the drop in $\Delta\nu$ is shifted to higher temperatures (~160 K); this indicates the slowest H motion, in agreement with the $R_1^H(T)$ data. For all phases of $Mg(BH_4)_2$, above the region of the sharp drop the proton line width stops to decrease, being nearly constant up to the highest temperature of our measurements. The substantial plateau value of $\Delta\nu$ indicates that the motion responsible for the observed line narrowing is indeed localized because such a motion leads to only partial averaging of dipole−dipole interactions between nuclear spins. It is interesting to note that the plateau value of $\Delta\nu$ for γ-$Mg(BH_4)_2$ is somewhat lower than that for α and β phases. This is consistent with high porosity of the γ phase which is expected to reduce the "intermolecular" dipole−dipole interactions not averaged by the reorientational motion. For parametrization of the proton spin−lattice relaxation data near the $R_1^H(T)$ peak in γ-$Mg(BH_4)_2$, we have used the same model with a Gaussian distribution of activation energies as for β-$Mg(BH_4)_2$. The results of such a simultaneous fit to the data in the range 230−320 K are shown by solid curves in Figure 2; the corresponding parameters are $\Delta M = (8.8 \pm 0.2) \times 10^9$ s^{-2}, $\tau_0 = (1.4 \pm 0.4) \times 10^{-13}$ s, $\bar{E}_a = 276 \pm 5$ meV, and $\Delta E_a = 19 \pm 4$ meV. Comparison with the fit parameters for β-$Mg(BH_4)_2$ shows that the average activation energy $\bar{E}_a$ for the γ phase is considerably larger, and the distribution width ΔE_a is smaller than for the β phase. The most probable value of the H jump rate τ^{-1} at 250 K derived from the fit parameters for γ-$Mg(BH_4)_2$ is 2×10^7 s^{-1}. For comparison, for β-$Mg(BH_4)_2$ the corresponding value of τ^{-1}(250 K) is approximately 10^{11} s^{-1}. It should be stressed, however, that while for the β phase the simple model with a Gaussian distribution of activation energies describes the behavior of $R_1^H(T)$ over the entire temperature range studied, for the γ phase this model describes only the data near the $R_1^H(T)$ peak. The experimental data for the γ phase suggest the presence of an additional motional process, giving a small frequency-dependent contribution to the relaxation rate at low temperatures. Such a process with a low apparent activation energy may correspond to the reorientation around the "easy" 2-fold axis nearly coinciding with the Mg−B−Mg line.[15] For the highly porous γ phase, the barrier for this type of reorientation is expected to be particularly small. Since γ-$Mg(BH_4)_2$ can adsorb nitrogen molecules[10] and the sample was sealed under ~500 mbar of N_2, we cannot exclude the presence of a certain amount of N_2 in the pores of the γ phase. However, the amount of the low-pressure gas in the sealed tube is negligible compared with the amount of the borohydride; therefore, we do not expect any significant effects due to possible N_2 adsorption on the parameters of the reorientational motion.

The ^{11}B spin−lattice relaxation rate R_1^B due to reorientational motion of BH_4 groups in borohydrides is dominated by the ^{11}B−^{1}H dipole−dipole contribution.[24,26] Therefore, the R_1^B measurements in borohydrides usually give essentially the same information on the parameters of reorientational motion as the R_1^H measurements. Figure 4 shows the results of the ^{11}B spin−lattice relaxation measurements for γ-$Mg(BH_4)_2$ at two resonance frequencies. Comparison of Figures 2 and 4 indicates that general features of the behavior of the ^{11}B relaxation rates in γ-$Mg(BH_4)_2$ are indeed similar to those of the proton relaxation rates. For parametrization of the R_1^B data near the $R_1^B(T)$ peak, we again use the model with a Gaussian distribution of activation energies. The description includes the ^{11}B analogue of eq 2 with

$$R_1^B(E_a) = \frac{\Delta M_{BH}\tau}{2}\left[\frac{1}{1+(\omega_B-\omega_H)^2\tau^2} + \frac{3}{1+\omega_B^2\tau^2} + \frac{6}{1+(\omega_B+\omega_H)^2\tau^2}\right] \quad (4)$$

and eq 1. The solid lines in Figure 4 show the simultaneous fits of the model to the data in the range 220−320 K; the resulting fit parameters are $\Delta M_{BH} = (7.0 \pm 0.2) \times 10^9$ s^{-2}, $\tau_0 = (1.4 \pm 0.4) \times 10^{-13}$ s, $\bar{E}_a = 276 \pm 5$ meV, and $\Delta E_a = 5 \pm 3$ meV. It should be noted that the values of the pre-exponential factor τ_0 and the average activation energy $\bar{E}_a$ coincide with the corresponding values derived from the ^{1}H relaxation data.

In contrast to the case of cubic alkali-metal borohydrides,[27] the reorientational motion of BH_4 groups in different phases of $Mg(BH_4)_2$ cannot be described in terms of a single activation energy. This may be related to the differences in coordination of the BH_4 groups. While in cubic alkali-metal borohydrides each BH_4 group has an ideal octahedral coordination by six metal ions, in all phases of $Mg(BH_4)_2$ each BH_4 group is nearly linearly coordinated by two Mg ions. As discussed in ref 15, such a linear coordination should lead to inequivalence of the barriers for BH_4 reorientations around different 2-fold and 3-fold axes. An additional complication is expected to arise from deviations from the ideal linear coordination characterized by the Mg−B−Mg angle of 180°. For β-$Mg(BH_4)_2$, there are five crystallographically inequivalent BH_4 groups with the Mg−B−Mg angles ranging from 149.5° to 166.0° in the experimental structure[8] and from 140.9° to 169.8° according to the DFT calculations.[29] It should be noted that recent DFT calculations[18] of the energy barriers for BH_4 reorientations in β-$Mg(BH_4)_2$ have revealed that the barriers for rotations around

dx.doi.org/10.1021/jp210509g | J. Phys. Chem. C 2012, 116, 4913−4920

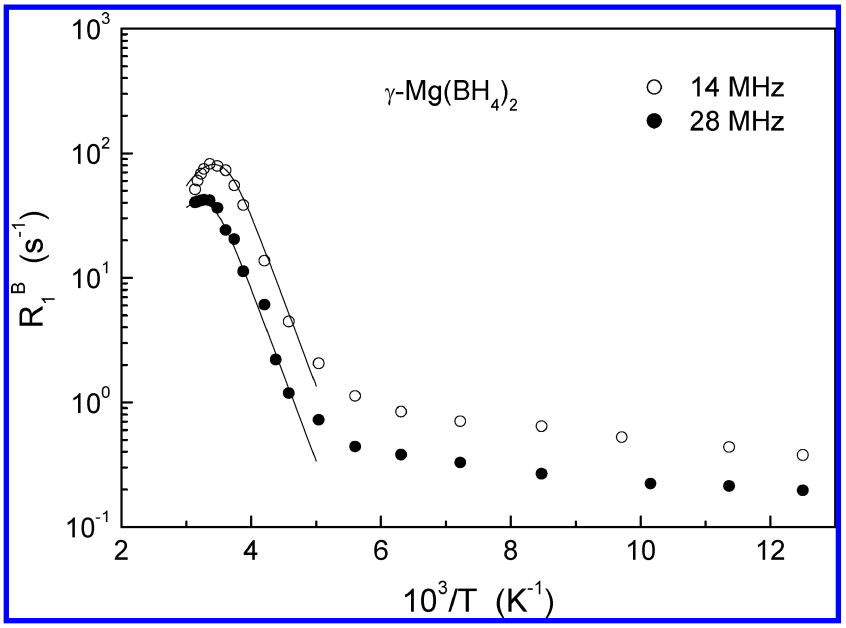

Figure 4. ^{11}B spin−lattice relaxation rates measured at 14 and 28 MHz for γ -$Mg(BH_4)_2$ as functions of the inverse temperature. The dashed lines show the simultaneous fits of the model with a Gaussian distribution of the activation energies to the data in the range 220−320 K.

the "easy" 2-fold axis are very sensitive to the actual Mg−B−Mg angle. Therefore, these calculations support the interpretation in terms of a broad distribution of the activation energies. For γ-$Mg(BH_4)_2$, all BH_4 groups are equivalent with the Mg−B−Mg angle of 177.1°.[10] However, the observed strong differences in the parameters of H jump motion for different phases of $Mg(BH_4)_2$ suggest the importance of subtle details of the local environment for the reorientational motion of BH_4 groups. It should be noted that gross features of the $R_1^H(T)$ dependences for α (ref 15) and γ phases of $Mg(BH_4)_2$ resemble each other (both have the main maximum near room temperature), while for the β phase the behavior of $R_1^H(T)$ is strongly different (the maximum is near 120 K). Apart from the Mg−H distances, we have to consider the H−H distances between BH_4 groups. These distances depend on the shape of the MgH_8 coordination polyhedra[10] in $Mg(BH_4)_2$. It has been found (see Table S6 in the Supporting Information of ref 10) that for α and γ phases the MgH_8 coordination polyhedra are identical and have a shape of the snub disphenoid (J_{84}) in notations of Johnson;[30] the resulting H−H distances are relatively short (~2.2−2.3 Å).[9] In contrast, the MgH_8 polyhedra for the β phase have different shapes: one Mg atom forms the biaugmented triangular prism (J_{50}), and the other one forms the gyrobifastigium (J_{26}),[10] both leading to slightly longer H−H distances. The difference in the H−H frameworks may give a key to understanding the difference between the reorientational behavior in α and γ phases of $Mg(BH_4)$ on one side and the β phase on the other.

2. α and β Phases of $Ca(BH_4)_2$. The results of the proton spin−lattice relaxation measurements for α-$Ca(BH_4)_2$ at three resonance frequencies are shown in Figure 5. As can be seen from this figure, $R_1^H(T)$ exhibits a frequency-dependent peak near 220 K. It should be noted that above ~160 K the observed recovery of nuclear spin magnetization is well described by a single exponential function; however, below 160 K the recovery deviates from the single-exponential behavior. The R_1^H values shown in Figure 5 at T < 160 K represent the results of a single-exponential fit to the experimental recovery curves; these values can be considered as some "average" parameters of the data. It

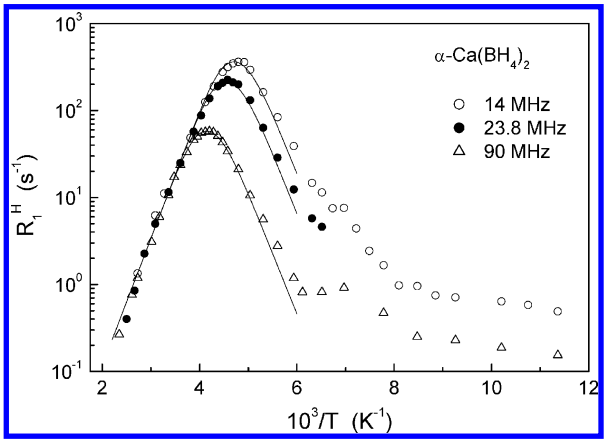

Figure 5. Proton spin−lattice relaxation rates measured at 14, 23.8, and 90 MHz for α-$Ca(BH_4)_2$ as functions of the inverse temperature. At T < 160 K the recovery of nuclear magnetization is nonexponential, and the data points in this range represent the results of single-exponential fits to the recovery curves. The solid lines show the simultaneous fits of the model with a Gaussian distribution of the activation energies to the data in the range 160−425 K.

is reasonable to assume that the deviations from the single-exponential relaxation at low temperatures originate from the presence of a minor β phase of $Ca(BH_4)_2$ in our sample (~13 wt %, according to X-ray diffraction analysis). It will be shown below that the proton spin−lattice relaxation rate for β-$Ca(BH_4)_2$ exhibits a peak near 120 K; therefore, the relaxation effects related to this minor phase should be more pronounced at low temperatures. Since the R_1^H data in Figure 5 below 160 K represent the results of a single-exponential fit to the nonexponential recovery curves, the exact position of the $R_1^H(T)$ "shoulder" in this figure may differ from the position of the relaxation peak for β-$Ca(BH_4)_2$. To evaluate the parameters of H jump motion in the α phase of $Ca(BH_4)_2$, we have analyzed the $R_1^H(T)$ results at T > 160 K using the model with a Gaussian distribution of activation energies (eqs 2, 3, and 1). The solid curves in Figure 5 show the results of the simultaneous

dx.doi.org/10.1021/jp210509g | J. Phys. Chem. C 2012, 116, 4913−4920

fit of this model to the data in the temperature range 160–425 K; the corresponding fit parameters are $\Delta M = (1.2 \pm 0.2) \times 10^{10}$ s^{-2}, $\tau_0 = (1.9 \pm 0.5) \times 10^{-15}$ s, $\bar{E}_a = 286 \pm 7$ meV, and $\Delta E_a = 12 \pm 4$ meV. It should be noted that in this case the distribution width appears to be quite small (about 4% of the average activation energy). This suggests that, in contrast to the case of β-Mg(BH$_4$)$_2$, the $R_1^H(T)$ data for α-Ca(BH$_4$)$_2$ can be satisfactorily described without any distribution of activation energies. Figure 6 shows the results of the ^{11}B spin–lattice

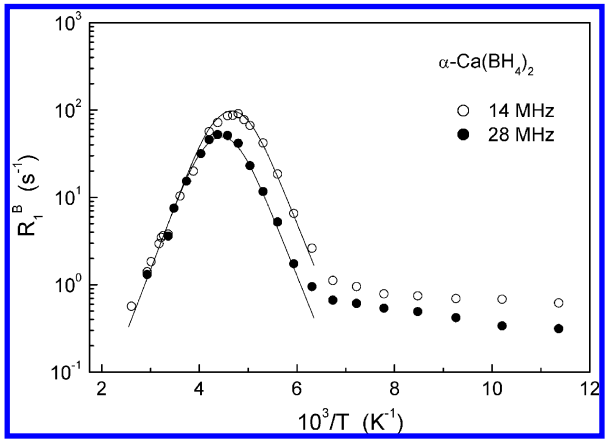

Figure 6. ^{11}B spin–lattice relaxation rates measured at 14 and 28 MHz for α-Ca(BH$_4$)$_2$ as functions of the inverse temperature. At $T < 160$ K the recovery of nuclear magnetization is nonexponential, and the data points in this range represent the results of single-exponential fits to the recovery curves. The solid lines show the simultaneous fits of the model with a Gaussian distribution of the activation energies to the data in the range 160–385 K.

relaxation measurements for α-Ca(BH$_4$)$_2$ at two resonance frequencies. It can be seen that general features of the behavior of the ^{11}B relaxation rates are similar to those of the ^{1}H relaxation rates. Below ~160 K, the recovery of the ^{11}B becomes nonexponential. In this range, the points shown in Figure 6 represent the results of a single-exponential fit to the experimental recovery curves. Above 160 K, the data points are expected to represent the intrinsic relaxation rates of the α phase of Ca(BH$_4$)$_2$. The solid curves in Figure 6 show the results of the simultaneous fit of the model with a Gaussian distribution of activation energies (the ^{11}B analogue of eq 2 and eqs 4 and 1) to the data in the temperature range 160–385 K. The resulting fit parameters are $\Delta M_{BH} = (9.2 \pm 0.4) \times 10^9$ s^{-2}, $\tau_0 = (1.5 \pm 0.4) \times 10^{-15}$ s, $\bar{E}_a = 285 \pm 6$ meV, and $\Delta E_a = 12 \pm 5$ meV. The motional parameters obtained from the ^{11}B relaxation data are very close to those derived from the ^{1}H relaxation data. Again, the resulting distribution width is small compared to the average activation energy.

The results of the proton spin–lattice relaxation measurements for β-Ca(BH$_4$)$_2$ at two resonance frequencies are shown in Figure 7. As can be seen from this figure, the temperature dependence of the ^{1}H spin–lattice relaxation rate exhibits a frequency-dependent peak near 120 K. The temperature of the $R_1^H(T)$ peak for the β phase of Ca(BH$_4$)$_2$ is considerably lower than that for α-Ca(BH$_4$)$_2$. This indicates that the reorientational motion of BH$_4$ groups in the β phase is generally much faster than in the α phase. It should be noted that the recovery of the ^{1}H spin magnetization for our sample of β-Ca(BH$_4$)$_2$ is well described by a single exponential function *below* ~170 K. Above 170 K, the observed recovery of the nuclear magnetization

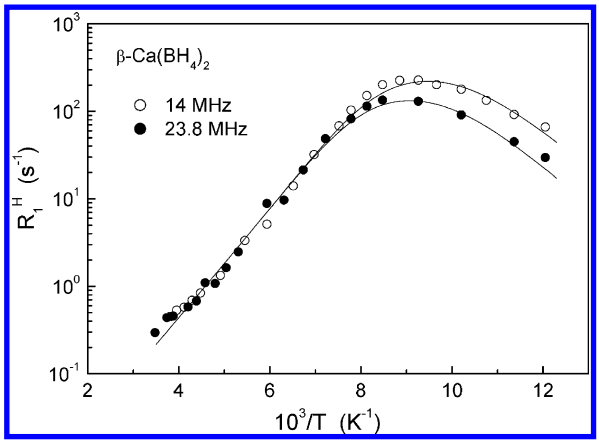

Figure 7. Proton spin–lattice relaxation rates measured at 14 and 23.8 MHz for β-Ca(BH$_4$)$_2$ as functions of the inverse temperature. At $T > 170$ K the recovery of nuclear magnetization is two-exponential, and the data points in this range represent the slower component of the recovery. The solid lines show the simultaneous fits of the model with a Gaussian distribution of the activation energies to the data.

can be satisfactorily described by two exponential terms. Furthermore, the faster component of the relaxation rate (not shown) is found to exhibit a maximum near 220 K. Comparison with the data shown in Figure 5 suggests that the faster component of the two-exponential recovery at $T > 170$ K originates from the presence of the α phase in our sample. This means that the $\alpha \rightarrow \beta$ transformation in the course of the annealing described in the Experimental Methods section was not complete. The fraction of the α phase estimated from the relative amplitudes of the two-exponential recovery is about 25%. This fraction is found to be stable during our measurements on β-Ca(BH$_4$)$_2$ (two days); therefore, there was no observable $\beta \rightarrow \alpha$ back transition in the course of these measurements. The fact that the $R_1^H(T)$ peaks in the α and β phases are observed at significantly differing temperatures allows us to separate the contributions from these phases. In Figure 7, the data points at $T > 170$ K correspond to the slower component of the two-exponential recovery. These points are expected to represent the intrinsic relaxation rates of the β phase; as can be seen from Figure 7, they form a smooth continuation of the low-temperature data. It is interesting to note that general features of the $R_1^H(T)$ behavior for the β phase of Ca(BH$_4$)$_2$ resemble those for the β phase of Mg(BH$_4$)$_2$ (see Figure 1). Therefore, for parametrization of the proton spin–lattice relaxation data for β-Ca(BH$_4$)$_2$, it is reasonable to use the same model with a Gaussian distribution of activation energies. The results of the simultaneous fit of this model to the data for β-Ca(BH$_4$)$_2$ are shown by the solid curves in Figure 7; the corresponding fit parameters are $\Delta M = (9.0 \pm 0.3) \times 10^9$ s^{-2}, $\tau_0 = (2.9 \pm 0.6) \times 10^{-14}$ s, $\bar{E}_a = 116 \pm 5$ meV, and $\Delta E_a = 11 \pm 3$ meV. Previous QENS studies of H jump motion in β-Ca(BH$_4$)$_2$ (ref 17) revealed two coexisting types of reorientational motion of BH$_4$ groups. The faster jump process with the activation energy of 100 meV was attributed to BH$_4$ reorientations around the 3-fold axes, and the slower process with the activation energy of 140 meV was ascribed to BH$_4$ reorientations around the 2-fold axes. Our value of the average activation energy, $\bar{E}_a = 116 \pm 5$ meV, lies between these two values derived from QENS measurements. The same is also true for the values of H jump rates at different temperatures. For example, at $T = 190$ K the most probable value of τ^{-1} derived from our fit

dx.doi.org/10.1021/jp210509g | J. Phys. Chem. C 2012, 116, 4913–4920

is 2.8×10^{10} s^{-1}; QENS measurements[17] at the same temperature yield τ^{-1} values of 5.9×10^{10} s^{-1} for the fast jump process and 4.1×10^{9} s^{-1} for the slower one. This comparison suggests that our NMR results for β-$Ca(BH_4)_2$ are in general agreement with QENS data for the reorientational motion in this compound. It should be noted that in some cases, when the ratio of the characteristic rates of two H jump processes is of the order of 10−50, the behavior of the measured proton spin−lattice relaxation rates may resemble that typical of a Gaussian distribution of activation energies. This was clearly demonstrated by comparison of NMR and QENS data for Laves-phase hydrides $ZrCr_2H_x$[31,32] where two H jump processes with different rates are known to coexist. Thus, our $R_1^H(T)$ results for β-$Ca(BH_4)_2$ do not exclude the presence of two frequency scales of reorientational motion in this compound. However, we have not found any signs of the *translational* H jump process reported in ref 17. Such a process would have led to the appearance of a very narrow component in proton NMR spectra; this feature has not been observed in our experiments. As was suggested by Blanchard et al.,[17] the translational H jump process in their sample was probably related to some interstitial impurities. The activation energies for BH_4 reorientations obtained from NMR and QENS measurements in alkaline-earth borohydrides are summarized in Table 1.

Table 1. Activation Energies for BH_4 Reorientations in Alkaline-Earth Borohydrides, As Derived from NMR and QENS Experiments[a]

compound	activation energy (meV)	dispersion of the E_a distribution (meV)	method	ref
α-$Mg(BH_4)_2$	116 (6), 198 (12), and 362 (5)	10 (4)	NMR	15
β-$Mg(BH_4)_2$	123 (4)		NMR	16
	39 (1), 76 (5), and 214 (4)		QENS	18
	138 (5)	36 (3)	NMR	this work
γ-$Mg(BH_4)_2$	276 (5)	19 (4)	NMR	this work
α-$Ca(BH_4)_2$	286 (7)	12 (4)	NMR	this work
β-$Ca(BH_4)_2$	100 and 140		QENS	17
	116 (5)	11 (3)	NMR	this work

[a]Uncertainties in the last digit are given in parentheses.

According to the structural studies,[12] each BH_4 group in α and β phases of $Ca(BH_4)_2$ is coordinated by three Ca ions which form a T-shaped arrangement around each B atom in the α phase and a nearly triangular arrangement in the β phase. In the α phase, the orientation of the BH_4 tetrahedron is such that it bridges three Ca ions via the tetrahedral edges. In the β phase, two Ca ions coordinate the BH_4 group via the edge and the third one via a tetrahedral vertex. The difference in the environment of BH_4 groups in α and β phases of $Ca(BH_4)_2$ suggests a difference in the parameters of the reorientational motion for these two crystalline modifications. It is interesting to note that a number of high-temperature borohydride phases are believed to be stabilized by an intrinsic orientational disorder. Such a disorder is found, for example, in the high-temperature phase of $LiBH_4$,[33] as well as in β-$Ca(BH_4)_2$.[12] This intrinsic disorder may contribute to the decrease in the barriers for reorientational BH_4 motion in the high-temperature phases via a formation of relatively shallow multiple-well potentials. As shown by Borgschulte et al.,[34] the librational modes in different phases of $Ca(BH_4)_2$ strongly affect the thermodynamic properties of these phases, determining their relative stability. Since BH_4 reorientations occur on a much lower frequency scale, the reorientational motion usually cannot be an interfering factor in vibrational spectroscopy or structure determination by diffraction methods. The exception is the case of nonideal reorientations, when a rotational jump does not lead to exactly the same configuration of a BH_4 group. Such a behavior has been found[24,35] for the high-temperature phase of $LiBH_4$; it results in the increase in the mean-square atomic displacement parameters seen by diffraction measurements.[33,36]

CONCLUSIONS

Our NMR results for different phases of $Mg(BH_4)_2$ indicate that the parameters of reorientational motion in α, β, and γ phases of this compound strongly differ from each other. In contrast to cubic alkali-metal borohydrides, the reorientational motion in different phases of $Mg(BH_4)_2$ cannot be described in terms of a single activation energy. Each of the phases is characterized by its own distinct distribution of the activation energies for BH_4 reorientations. The fastest reorientational motion is observed for β-$Mg(BH_4)_2$. Since in all phases of $Mg(BH_4)_2$ the BH_4 groups are coordinated by two Mg ions in a nearly linear configuration, our results indicate the importance of subtle details of local environment for the parameters of H jump motion. Such details are likely to include a spread in the B−Mg distances and Mg−B−Mg angles, as well as the H−H distances between different BH_4 groups. As in the case of $Mg(BH_4)_2$ phases, the parameters of reorientational motion in α and β phases of $Ca(BH_4)_2$ strongly differ from each other, and the β phase shows much faster motion than the α phase. The observed low barriers for BH_4 reorientations in the high-temperature (β) phases of both systems may be related to the intrinsic orientational disorder of BH_4 groups in these phases. However, for β-$Ca(BH_4)_2$ we have not found any signs of the translational H jump process reported previously[17] on the basis of QENS measurements.

AUTHOR INFORMATION

Corresponding Author

*E-mail: skripov@imp.uran.ru (A.V.S.); yaroslav.filinchuk@uclouvain.be (Y.F.). Fax: +7-343-374-5244 (A.V.S.); +32-10-47-2707 (Y.F.).

Notes

The authors declare no competing financial interest.

ACKNOWLEDGMENTS

This work was partially supported by the Priority Program "Basics of development of energy systems and technologies" of the Russian Academy of Sciences, the Swiss National Science Foundation, the Danish National Research Foundation (Center for Materials Crystallography), and the Danish Strategic Research Council (Center for Energy Materials).

REFERENCES

(1) Nakamori, Y.; Miwa, K.; Ninomiya, A.; Li, H.; Ohba, N.; Towata, S.; Züttel, A.; Orimo, S. *Phys. Rev. B* **2006**, *74*, 045126.

(2) Miwa, K.; Aoki, M.; Noritake, T.; Ohba, N.; Nakamori, Y.; Towata, S.; Züttel, A.; Orimo, S. *Phys. Rev. B* **2006**, *74*, 155122.

(3) Li, H. W.; Yan, Y.; Orimo, S.; Züttel, A.; Jensen, C. M. *Energies* **2011**, *4*, 185.

(4) Barkhordarian, G.; Jensen, T. R.; Doppiu, S.; Rösenberg, U.; Borgschulte, A.; Gremaud, R.; Cerenius, Y.; Dornheim, M.; Klassen, T.; Bormann, R. *J. Phys. Chem. C* **2008**, *112*, 2743.

(5) Severa, G.; Rönnebro, E.; Jensen, C. M. *Chem. Commun.* **2010**, *46*, 421.
(6) Newhouse, R. J.; Stavila, V.; Hwang, S.-J.; Klebanoff, L. E.; Zhang, J. Z. *J. Phys. Chem. C* **2010**, *114*, 5224.
(7) Černý, R.; Filinchuk, Y.; Hagemann, H.; Yvon, K. *Angew. Chem., Int. Ed.* **2007**, *46*, 5765.
(8) Her, J.-H.; Stephens, P. W.; Gao, Y.; Soloveichik, G. L.; Rijssenbeek, J.; Andrus, M.; Zhao, J.-C. *Acta Crystallogr. B* **2007**, *63*, 561.
(9) Filinchuk, Y.; Černý, R.; Hagemann, H. *Chem. Mater.* **2009**, *21*, 925.
(10) Filinchuk, Y.; Richter, B.; Jensen, T. R.; Dmitriev, V.; Chernyshov, D.; Hagemann, H. *Angew. Chem., Int. Ed.* **2011**, *50*, 11162.
(11) Buchter, F.; Łodziana, Z.; Remhof, A.; Friedrichs, O.; Borgschulte, A.; Mauron, P.; Züttel, A.; Sheptyakov, D.; Barkhordarian, G.; Bormann, R.; Chłopek, K.; Fichtner, M.; Sørby, M.; Riktor, M.; Hauback, B.; Orimo, S. *J. Phys. Chem. B* **2008**, *112*, 8042.
(12) Filinchuk, Y.; Rönnebro, E.; Chandra, D. *Acta Mater.* **2009**, *57*, 732.
(13) Buchter, F.; Łodziana, Z.; Remhof, A.; Friedrichs, O.; Borgschulte, A.; Mauron, P.; Züttel, A.; Sheptyakov, D.; Palatinus, L.; Chłopek, K.; Fichtner, M.; Barkhordarian, G.; Bormann, R.; Hauback, B. *J. Phys. Chem. C* **2009**, *113*, 17223.
(14) Fichtner, M.; Chłopek, K.; Longhini, M.; Hagemann, H. *J. Phys. Chem. C* **2008**, *112*, 11575.
(15) Skripov, A. V.; Soloninin, A. V.; Babanova, O. A.; Hagemann, H.; Filinchuk, Y. *J. Phys. Chem. C* **2010**, *114*, 12370.
(16) Shane, D. T.; Rayhel, L. H.; Huang, Z.; Zhao, J. C.; Tang, X.; Stavila, V.; Conradi, M. S. *J. Phys. Chem. C* **2011**, *115*, 3172.
(17) Blanchard, D.; Riktor, M. D.; Maronsson, J. B.; Jacobsen, H. S.; Kehres, J.; Sveinbjörnsson, D.; Bardaji, E. G.; Léon, A.; Juranyi, F.; Wuttke, J.; Hauback, B. C.; Fichtner, M.; Vegge, T. *J. Phys. Chem. C* **2010**, *114*, 20249.
(18) Blanchard, D; Maronsson, J. B.; Riktor, M. D.; Kheres, J; Sveinbjörnsson, D.; Bardaji, E. G.; Léon, A.; Juranyi, F.; Wuttke, J.; Lefmann, K; Hauback, B. C.; Fichtner, M.; Vegge, T. *J. Phys. Chem. C* **2012**, *116*, 2013.
(19) Abragam, A. *The Principles of Nuclear Magnetism*, Clarendon Press: Oxford, 1961.
(20) Tsang, T.; Farrar, T. C. *J. Chem. Phys.* **1969**, *50*, 3498.
(21) Niemelä, L; Ylinen, E. *Phys. Lett.* **1970**, *31A*, 369.
(22) Tarasov, V. P.; Bakum, S. I.; Privalov, V. I.; Shamov, A. A. *Russ. J. Inorg. Chem.* **1990**, *35*, 1035.
(23) Tarasov, V. P.; Bakum, S. I.; Privalov, V. I.; Shamov, A. A. *Russ. J. Inorg. Chem.* **1990**, *35*, 2096.
(24) Skripov, A. V.; Soloninin, A. V.; Filinchuk, Y.; Chernyshov, D. *J. Phys. Chem. C* **2008**, *112*, 18701.
(25) Corey, R. L.; Shane, D. T.; Bowman, R. C.; Conradi, M. S. *J. Phys. Chem. C* **2008**, *112*, 18706.
(26) Babanova, O. A.; Soloninin, A. V.; Stepanov, A. P.; Skripov, A. V.; Filinchuk, Y. *J. Phys. Chem. C* **2010**, *114*, 3712.
(27) Babanova, O. A.; Soloninin, A. V.; Skripov, A. V.; Ravnsbæk, D. B.; Jensen, T. R.; Filinchuk, Y. *J. Phys. Chem. C* **2011**, *115*, 10305.
(28) Markert, J. T.; Cotts, E. J.; Cotts, R. M. *Phys. Rev. B* **1988**, *37*, 6446.
(29) Dai, B.; Sholl, D. S.; Johnson, J. K. *J. Phys. Chem. C* **2008**, *112*, 4391.
(30) Johnson, N. W. *Can. J. Math.* **1966**, *18*, 169.
(31) Skripov, A. V.; Belyaev, M.Yu. *J. Phys.: Condens. Matter* **1993**, *5*, 4767.
(32) Skripov, A. V.; Pionke, M.; Randl, O.; Hempelmann, R. *J. Phys.: Condens. Matter* **1999**, *11*, 1489.
(33) Filinchuk, Y.; Chernyshov, D.; Černý, R. *J. Phys. Chem. C* **2008**, *112*, 10579.
(34) Borgschulte, A.; Gremaud, R.; Züttel, A.; Martelli, P.; Remhof, A.; Ramirez-Cuesta, A. J.; Refson, K.; Bardaji, E. G.; Lohstroh, W.; Fichtner, M.; Hagemann, H.; Ernst, M. *Phys. Rev. B* **2011**, *83*, 024102.
(35) Verdal, N.; Udovic, T. J.; Rush, J. J. *J. Phys. Chem. C* **2012**, *116*, 1614.
(36) Hartman, M. R.; Rush, J. J.; Udovic, T. J.; Bowman, R. C.; Hwang, S.-J. *J. Solid State Chem.* **2007**, *180*, 1298.